J|A|C|S
ARTICLES
Published on Web 09/21/2006

Assisted Desolvation as a Key Kinetic Step for Crystal Growth

Stefano Piana, Franca Jones, and Julian D Gale*

Contribution from the Nanochemistry Research Institute, Curtin University of Technology, GPO Box U1987, 6845 Perth, WA. Australia

Received July 3, 2006; E-mail: julian@ivec.org

Abstract: The crystallization of materials from a supersaturated solution is a fundamental chemical process. Although several very successful models that provide a qualitative understanding of the crystal growth process exist, in most cases the atomistic detail of crystal growth is not fully understood. In this work, molecular dynamics simulations of the morphologically most important surfaces of barite in contact with a supersaturated solution have been performed. The simulations show that an ordered and tightly bound layer of water molecules is present on the crystal surface. The approach of an ion to the surface requires desolvation of both the surface and the ion itself leading to an activated process that is rate limiting for two-dimensional nucleation to occur. However, desolvation on specific surfaces can be assisted by anions adsorbed on the crystal surface. This hypothesis, corroborated by crystallization and scanning electron microscopy studies, allows the rationalization of the morphology of barite crystals grown at different supersaturations.

Introduction

Although crystallization is an industrially useful means of purifying and/or separating solids, not all crystallization is desirable. Unwanted crystallization is known as "scale formation" and causes problems within industrial processing units.[1−3] Barium sulfate is a common and persistent scale in the offshore oil production industry where changes in temperature, pressure, and mixing of different water streams cause barite to precipitate.[4,5]

Considerable scientific effort has been devoted to studying barium sulfate on both a fundamental level and from an industrial perspective. Atomic force microscopy (AFM) studies from Putnis and co-workers[6−9] have shown that up to moderate supersaturations two-dimensional nucleation on the barium sulfate surface occurs at a negligible rate, and screw dislocations are mostly responsible for crystal growth. The 2D nuclei formed are highly asymmetric and their shape, size, and the rate at which they grow on the different faces of the crystal have been correlated with the energy of incorporation of growth units at steps. However, a fundamental understanding of the kinetics of 2D nucleation and how the kinetics impact on the crystal morphology is still lacking.

It is well-known that the solvent can have a strong effect on the energetics of crystallization.[10−12] The idea that ion desolvation may be an important kinetic step in the crystal growth of polyelectrolytes was introduced about 20 years ago with the work of Nielsen.[13,14] However, the systematic study of solvent effects on the crystallization of inorganic solids has received little experimental attention. From an experimental perspective, Amsler[15] studied potassium chloride precipitation in water and water/ethanol mixtures as far back as 1942. Similarly, Seo et al.[16] have investigated the precipitation of calcium carbonate from ethanol mixtures. However, this later work was not really a study of solvent effects but an investigation of the influence of supersaturation on the precipitation of different polymorphs. Despite several studies, it remains difficult to obtain unambiguous insights into the role of solvation in the growth of inorganic materials from experiment alone.

Computer simulations can prove to be a very useful compliment to experiment in determining the atomistic detail of the kinetics of crystallization. However, few investigations have been reported that take the effect of solvent fully into account.[17−21]

(1) Bott, T. R. In *Fouling of Heat Exchangers*; Elsevier: Amsterdam, The Netherlands 1995.
(2) Mackay, E. *Trans Inst. Chem. Eng.* **2003**, *81* (A), 326−332.
(3) Hamed, O. A.; Al-Sofi, M. A. K.; Imam, M.; Ba Mardouf, K.; Al-Mobayed, A. S.; Ehsan, A. *Desalination* **2000**, *128*, 275−280.
(4) Graham, G. M.; Boak, L. S.; Sorbie, K. S. *The Influence of Formation Calcium on the Effectiveness of Generically Different Barium Sulfate Oilfield Scale Inhibitors*; Heriot-Watt University: U.K., 1997; p 611−626.
(5) Sorbie, K. S.; Mackay, E. *J. Pet. Sci. Eng.* **2000**, *27*, 85−106.
(6) Pina, C. M.; Putnis, C. V.; Becker, U.; Biswas, S.; Carroll, E. C.; Bosbach, D.; Putnis, A. *Surf. Sci.* **2004**, *553*, 61.
(7) Pina, C. M.; Becker, U.; Risthaus, P.; Bosbach, D.; Putnis, A. *J. Cryst. Growth* **1998**, 187, 119−125.
(8) Bosbach, D.; Hall, C.; Putnis, A. *Chem. Geol.* **1998**, *151*, 143−160.
(9) Pina, C. M.; Becker, U.; Risthaus, P.; Bosbach, D.; Putnis, A. *Nature* **1998**, *395*, 483−486.
(10) de Leeuw, N. H.; Parker, S. C. *J. Phys. Chem. B* **1998**, *102*, 2914−2922.
(11) Bennema, P. *J. Cryst. Growth* **1992**, *122*, 110−119.
(12) Lahav, M.; Leiserowitz, L. *Chem. Eng. Sci.* **2001**, *56*, 2245−2253.
(13) Nielsen, A. E. *J. Cryst. Growth* **1984**, *67*, 289−310.
(14) Nielsen, A. E.; Toft, J. M. *J. Cryst. Growth* **1984**, *67*, 278−288.
(15) Amsler, J. *Helv. Phys. Acta* **1942**, *15*, 699−732.
(16) Seo, K.-S. H. C.; Wee, J.-H.; Park, J.-K.; Ahn, J.-W. *J. Cryst. Growth* **2005**, *276*, 680−687.
(17) Piana, S.; Gale, J. *J. Am. Chem. Soc.* **2005**, *127*, 1975−1982.
(18) Liu, X. Y.; Boek, E. S.; Briels, W. J.; Bennema, P. *Nature* **1995**, *374*, 342−345.
(19) Anwar, J.; Boateng, P. K. *J. Am. Chem. Soc.* **1998**, *120*, 9600−9604.
(20) Hussain, M.; Anwar, J. *J. Am. Chem. Soc.* **1999**, *121*, 8583−8591.
(21) Kerisit, S.; Parker, S. C. *J. Am. Chem. Soc.* **2004**, *126*, 10152−10161.

10.1021/ja064706q CCC: $33.50

The impact of solvent on crystal growth can sometimes be predicted by continuum models, especially when only the thermodynamics of the process is being examined, but has rarely been the subject of rigorous theoretical investigations because of the inherent complexity of dealing with a system with many degrees of freedom, such as the solvent-crystal interface. We thus present a study based on the molecular dynamics (MD) simulation of the barite crystal surface in contact with a supersaturated solution. There has been one prior work in this area by Jang et al.[22] where barite was the system of interest and solvation by water using a molecular dynamics approach was attempted. This work showed that the surface energies of the barite faces were ordered as follows: $(010) \approx (210) < (001)$. However, this ordering of surface energies is inconsistent with the morphology of barium sulfate, particularly for barite formed at low supersaturation. This raises the question of whether consideration of the thermodynamics is sufficient to understand the formation of materials such as barite or whether the kinetics might be the dominant influence? The aim of this study is to address this issue and to focus on the specific role of the solvent.

The present theoretical investigation indicates that the crystal surface is covered with a layer of tightly bound water molecules. This layer provides an effective activation barrier to nucleation such that it prevents the cations in solution from reaching the crystal surface. This is consistent with the hypothesis, based on experimental[13,23] and theoretical[21] work, that desolvation of the surface, and of the cations, can be a rate-determining kinetic step in crystal growth. However, we observe that the barrier for the diffusion of anions to the crystal surface is much smaller and that anions can very effectively catalyze the cation desolvation. This process is surface specific, thus providing the key to explaining the differences in the growth rates of surfaces that are thermodynamically very similar. Crystal growth experiments have been performed to corroborate these findings.

Methodology

Optimization of a Force Field To Describe the Barite−Water Interface. The only force field reported in the literature that has been created to specifically describe the water−barite interface[22] has a complex functional form that has not been widely implemented. Furthermore, this force field has not been optimized to correctly reproduce the properties of the barium and sulfate ions in solution. For this reason, as a first step of the investigation, a force field has been developed to describe the barite−water interaction with a functional form that is composed of electrostatic interactions supplemented by a Lennard-Jones description of the short-ranged potential.

The starting parameters for the sulfate ion were taken from the GROMOS force field.[24] In this force field, the charges on the atoms were +2 for the Ba ion, −0.635 for the sulfate oxygen atoms, and +0.540 for sulfur. The equilibrium structural parameters for the sulfate ion were taken to be 0.15 nm for the S−O bond length and the tetrahedral angle of 109.47 degrees for O−S−O. The functional form for the bond angle was the GROMOS96 form with a force constant of 1295.39 kJ mol^{-1}. These parameters were not modified, while the Lennard-Jones (LJ) parameters of the barium and sulfate ions were fitted using the program GULP[25] to thermodynamic and structural data, namely, the lattice energy, the cell parameters, the fractional coordinates, and the elastic constants of the crystalline material. Subsequently, the parameters that describe the interaction between the ions and water were tuned in order to reproduce the main peaks in the experimental radial distribution function in solution and the experimental enthalpy of hydration of the two ions. The LJ parameters obtained from this procedure and used in the present work are reported in Table 1.

Table 1. Lennard-Jones Coefficients C_6 and C_{12} Used in the Present Work to Describe the Interactions within Barite and between Both Barium and Sulfate Ions with Water

atom pair	C_6 (kJ mol^{-1} nm^6)	C_{12} (kJ mol^{-1} nm^{12})
$O_{water}-S_{SO_4}$	0.000	5.583×10^{-6}
$O_{water}-O_{SO_4}$	0.000	3.200×10^{-6}
$O_{water}-Ba$	0.008	5.359×10^{-6}
$S_{SO_4}-S_{SO_4}$	0.000	0.000
$S_{SO_4}-O_{SO_4}$	0.000	0.000
$S_{SO_4}-Ba$	0.000	6.470×10^{-5}
$O_{SO_4}-O_{SO_4}$	0.000	0.000
$O_{SO_4}-Ba$	0.000	2.571×10^{-6}
Ba−Ba	0.000	0.000

Table 2. Comparison between the Experimental and Calculated Properties of Both Barite and the Component Ions in Dilute Aqueous Solution

property	experimental[h]	calculated[h]
cell parameters *a*,*b*,*c* (nm)	0.888,[a] 0.546,[a] 0.716[a]	0.879, 0.545, 0.705
cell angles α, β, γ (deg)	90.0,[a] 90.0,[a] 90.0[a]	90.0, 90.0, 90.0
lattice energy (kJ mol^{-1})	−2476 (50)[b]	−2463 (5)
ΔH_{hyd} Ba^{2+} (kJ mol^{-1})	−1314,[c] −1339,[d] −1362[e]	−1360 (10)
ΔH_{hyd} SO_4^{2-} (kJ mol^{-1})	−1138(50),[c] −1109(50)[d]	−1109 (10)
$d(O_{wat}\cdots Ba^{2+}_{(hyd)})$ (nm)	0.281 (0.003)[f]	0.275
$d(O_{wat}\cdots O_{SO4(hyd)})$ (nm)	0.28 (0.001)[g]	0.29
N_{wat} (Ba^{2+})	8.1(3)[f]	8.8

[a] Ref 28 [b] Ref 22 [c] Ref 29 [d] Ref 30 [e] Ref 31 [f] Ref 32 [g] Ref 33 [h] Errors are reported in parentheses where available.

The difference between the calculated and the experimental values based on the final parameter set are reported in Table 2. The radial distribution function and the enthalpy of hydration at 298.15 K were calculated for a system composed of one ion and 894 water molecules in a 3.0 nm × 3.0 nm × 3.0 nm cubic box. A constant pressure (NPT) MD simulation for 2 ns was performed for each system, and the last 1.5 ns were used for data analysis. The enthalpy of hydration was calculated as the difference between the MD averaged value obtained from the last 1.5 ns of simulation and the average energy of a box of 894 water molecules simulated under the same conditions. A control simulation performed with a larger 5.0 nm × 5.0 nm × 5.0 nm box containing 4179 water molecules gave unchanged results. The number of water molecules in the first coordination shell (N_{wat}) was calculated by integration of the first peak of the ion−water radial distribution function. The water residence time in the first hydration shell (τ_{wat} = 132(10) ps) was calculated as in ref 26. This value corresponds to a rate constant for the dissociation from the first hydration sphere of 7.6 × 10^{-9} s^{-1} that is in line with the experimental value of 10^{-9}−10^{-10} reported in the literature.[27]

While the radial density distribution function and overall thermodynamics of ion solvation are key indicators of force field quality for the present work, it is important to consider whether the details of the water−surface interaction are correctly described too. To this end, the parameters were then further validated by performing ab initio calculations of the structure and energy of interaction of water molecules

(22) Jang, Y. H.; Chang, X. Y.; Blanco, M.; Hwang, S.; Tang, Y.; Schuler, P.; Goddard, W. A., III. *J. Phys. Chem. B* **2002**, *106*, 9951−9966.
(23) Dove, P. M.; Czank, C. A. *Geochim. Cosmochim. Acta* **1995**, *59* (10), 1907−1915.
(24) Van Gusteren, W. F.; Billeter, S. R.; Eising, A. A.; Hunenberger, P. H.; Kruger, P. K. H. C.; Mark, A. E.; Scott, W. R.; Tironi, I. G. *Biomolecular Simulation: The GROMOS96 Manual and User Guide*; Hochschulverlag AG: Zurich, Switzerland, 1996.
(25) Gale, J. D.; Rohl, A. L. *Mol. Simul.* **2003**, *29*, 291−341.
(26) Impey, R. W.; Madden, P. A.; McDonald, I. R. *J. Phys. Chem.* **1983**, *87*, 5071−5083.
(27) Hofer, T. S.; Rode, B. M.; Randolf, B. R. *Chem. Phys.* **2005**, *312*, 81−88.

Table 3. Binding Energies (in kJ/mol) Per Molecule for Water as a Function of Coverage on the Barite (001) Surface[a]

binding site and number of waters	ab initio binding energy	ab initio binding energy with C6 correction	force field binding energy
low/1	−55.1	−73.9	−78.2
low/2	−54.1	−72.5	−70.5
high/1	−65.1	−85.1	−95.6
high/2	−56.8	−73.6	−92.4
low and high/4	−53.2	−71.0	−82.1

[a] Values are calculated with nonlocal density-functional theory with the PBE functional and with the force field described in the present work.

on the (001) surface of barite. For this purpose, density-functional theory calculations, based on the generalized gradient approximation of Perdew, Burke, and Ernzerhof,[34] were performed using the SIESTA methodology and software.[35] Norm conserving pseudopotentials of the Troullier−Martins form[36] were used to represent the nonlocal potential due to the nucleus and core electrons, while the valence Kohn−Sham eigenstates were described with soft-confined basis sets of double-ζ quality with polarization functions. The electron density was represented using an auxiliary real-space mesh with a kinetic energy cutoff of 200 Ry.

The bulk structure of barite was optimized at constant pressure, and then a slab containing five layers was created to represent the (001) surface of the material, which represents a thickness of approximately 35 Å. A vacuum gap of 25 Å was then placed above the surface, such that the interaction between images of the slabs was negligible. After full relaxation of the slab, water was adsorbed in a number of configurations above the surface. Assuming that the water preferentially solvates the barium ions at the surface, which is consistent with the solvation energies of the ions, the adsorbate can bind to one of two distinct metal atoms. These sites we will refer to as high and low to reflect the fact that the former barium ion is much closer to the surface than the other. A 2×1 supercell was created so that four cations were present on the surface, two of each kind, so that a range of concentrations of water could be adsorbed.

Binding energies calculated for one, two, or four water molecules adsorbed on the (001) surface of barite are given in Table 3. A comparison of the force field results with those from nonlocal density functional, corrected for basis set superposition error using the counterpoise method, is presented. In comparing the energies, we apply a further correction to allow for the fact that the density-functional calculation fails to account for the attractive C6 dispersion contribution in the long-range limit. To achieve this, a single point calculation is performed at the optimized ab initio geometry to compute the C6 only contribution as a pairwise interaction with parameters taken from the force field (see above).

It appears that the present force field performs a reasonable job of capturing the interactions between the barium sulfate and the adsorbed water, considering that the force field was primarily parametrized against the dilute solution solvation of the separate ions. The water is especially well described when bound near to the barium that is lower within the surface, with the energy differences being within the uncertainties of the density-functional calculation. The preference for binding near to the higher barium is captured, though the magnitude of the energy change is exaggerated. This is due to the strong barium-water dispersion interaction, also reflected by the large value of C6 (Table 1). Indeed, self-consistent inclusion of the C6 term during the geometry optimization in the ab initio method would reduce this discrepancy and particularly affect this site. In terms of the geometries, the orientation of the water is very similar between the density-functional results and the force field, with just slight adjustments in the rotation of the water being observed in most cases. The one exception is that at high coverages, the force field energy minimization drops into a different minimum when starting from the ab initio structure, with the cell parameters rescaled to the correct values. In this case, the water from the high barium site moves so as to hydrogen bond to one of the other water molecules.

Initial attempts to derive a force field for the water−barite interaction yielded qualitatively different structures for water adsorbed on the surface in comparison to the quantum mechanical results. Hence, given the complexity of the system and the limited reliable data to compare to, the results from the present model are considered satisfactory for simulation of the solvated surface.

Molecular Dynamics Simulations of the Barite−Water Interface. Molecular dynamics simulations of the three morphologically most important faces, (001), (210), and (010), in contact with pure SPC water were performed with the program GROMACS[37] using the force field described in the previous section. Starting structures were generated employing the crystallographic unit cell of barite as a template. The program GDIS[38] was used to generate 6×4, 4×4, and 4×4 2D periodic (001), (210), and (010) surface supercells, respectively. The surfaces were 4, 6, and 4 layers deep and were transformed into 3D periodic systems by extending the cell axis in the *z* direction. The empty space in the simulation cell was filled with water molecules. A total of 2266, 729, and 904 water molecules were required to solvate the (001), (210), and (010) surfaces, respectively. All bonds lengths were constrained to their equilibrium values with the LINCS algorithm.[39] Nonbonded interactions were evaluated out to a cutoff of 1.2 nm and the particle mesh Ewald method[40] was used to treat the long-range electrostatic interactions. The time step for the simulations was 2 fs and the nonbonded pair list was updated every five steps. Constant temperature simulations at 218.15 K were performed by coupling the system to a Nose−Hoover thermostat[41] with a relaxation time of 3.0 ps. Constant pressure was obtained by coupling to an anisotropic Berendsen barostat[42] with relaxation time of 5.0 ps. The compressibility of the system was set to 4.5×10^{-5} bar^{-1} in the *z* direction and 5.0×10^{-6} bar^{-1} in the *x* and *y* directions. All systems were equilibrated by performing 20 ps of NVT simulation at 298K. Subsequently, 4 ns of NPT simulation at 298 K was performed, and the last 3 ns were used for data analysis. Surface energies were calculated as the difference between the MD-averaged potential energy of the barite + water system and the same quantity determined separately for bulk water and bulk barite.

Molecular Dynamics Simulations of 2D Nucleation. Molecular dynamics simulations of the three morphologically most important faces, (001), (210), and (010), in contact with a supersaturated solution were performed. The starting structures for the systems were generated as for the previous simulations with the difference that each system was solvated with a 1 M solution of Ba^{2+} and SO_4^{2-} ions. All systems were equilibrated by performing 100 ps of NVT simulation at 298 K followed

(28) Hill, R. J. *Can. Mineral.* **1977**, *15*, 522−526.
(29) Marcus, Y. *Ion Solvation*; John Wiley and Sons: New York, 1985.
(30) Vasilev, V. P.; Zolotarev, E. K.; Kapustinskii, A. F.; Mischenko, K. P.; Podgornaya, E. A.; Yatsimirskii, K. B. *Zh. Fiz. Khim.* **1960**, *34* (8), 1762−1767.
(31) Noyes, R. M. *J. Am. Chem. Soc.* **1962**, *84*, 513−522.
(32) Persson, I.; Sandstorm, M.; Yokoyama, H.; Chaudhry, M. *J. Phys. Sci.* **1995**, *50* (1), 21−37.
(33) Marques, M. A.; Cabaço, M. I.; de Barros Marques, M. I.; Gaspar, A. M. *J. Phys.: Condens. Matter* **2002**, *14*, 7427−7448.
(34) Perdew, J. P.; Burke, K.; Ernzerhof, M. *Phys. Rev. Lett.* **1996**, *77*, 3865−3868.
(35) Soler, J. M.; Artacho, E.; Gale, J. D.; Garcia, A.; Junquera, J.; Ordejon, P.; Sanchez-Portal, D. *J. Phys.: Condens. Matter* **2002**, *14*, 2745−2779.
(36) Troullier, N.; Martins, J. L. *Phys. Rev. B: Condens. Matter Mater. Phys.* **1991**, *43*, 1943−2006.
(37) Lindhal, E.; Hess, B.; van der Spoel, D. *J. Mol. Model.* **2001**, *7*, 306−317.
(38) Fleming, S. D.; Rohl, A. L. *Z. Kristallogr.* **2004**.
(39) Hess, B.; Bekker, H.; Berendsen, H. J. C.; Fraaije, G. E. M. *J. Comp. Chem.* **1997**, *18*, 1463−1472.
(40) Essman, U.; Perera, L.; Berkowitz, M. L.; Darden, T. A.; Lee, H.; Pedersen, L. G. *J. Chem. Phys.* **1995**, *103*, 8577−8593.
(41) Hoover, W. G. *Phys. Rev. A: At., Mol., Opt. Phys.* **1985**, *31*, 1695−1697.
(42) Berendsen, H. J. C.; Postma, J. P. M.; van Gunsteren, W. F.; DiNola, A.; Haak, J. R. *J. Chem. Phys.* **1984**, *81*, 3684−3690.

by 104 ns of NPT simulation at 298 K and 1 atm. The last 100 ns were used for data analysis.

Umbrella Sampling Simulations. Analogously to previous studies on the adsorption of cations on the surface of calcite,[21] the free energy profile for the adsorption of a Ba^{2+} ion on the crystal surface was calculated with the umbrella sampling approach. In these calculations, the distance between Ba^{2+} and the crystal surface was fixed with a harmonic constraint. The force acting on the constraint at different distances was calculated with molecular dynamics simulations and used to reconstruct the adsorption free energy. Two sets of umbrella sampling simulations were performed where the distance between a Ba^{2+} ion and the crystal surface was progressively reduced from ~0.6 to ~0.1 nm. Starting points for all the simulations were the same systems used for the barite−water interface calculations. In the first set of calculations a barium ion was added to the solution, whereas in the second set both a barium ion and a sulfate ion were added to the solution. The starting position of the sulfate ion was located on the crystal surface. Ten simulations were performed where the position of the barium ion was constrained at distances ranging between 0.1 and 0.6 nm from the crystal surface. The constraint force was 3000 kJ mol^{-1} nm^{-1} and 1.2 ns of constrained MD simulation was performed for each system, with the last 800 ps of each simulation being used for data analysis. The reaction free energy was calculated from the simulation using the weighted histogram analysis method.[43]

Crystallization of Barite from Water and Methanol. To perform crystallization experiments in methanol/water mixtures, knowledge of the solubility of barium sulfate in the solvent was required. To this end, freshly precipitated barium sulfate, formed by mixing AR grade Na_2SO_4 and $BaCl_2$ in milliQ water, was filtered and thoroughly washed to remove traces of residual salt. These solids were then dried in a desiccator for ~1 week. The "pure" barium sulfate was added to 500 mL of solvent (100% H_2O, 75% H_2O, 40% H_2O, and 0% H_2O) in excess and placed in a thermostated bath (25 ± 0.1 °C) with shaker table. After more than one week of equilibration an aliquot was removed and filtered through a 0.2 μm filter membrane, and 10 mL of this filtrate was evaporated to dryness (to avoid methanol contamination in the ICP instrument). The dried sample was placed in an oven at 50 °C to remove all traces of methanol, and then 10 mL of 5% HNO_3 was added before the Ba and S content was measured using ICP. These values were then used to calculate K_{sp} (the solubility product) for each of the solutions. Four replicates for each of the four solutions were used to obtain a relationship between the methanol content and the barium sulfate equilibrium solubility product (shown in Supporting Information). This K_{sp} value was then used to calculate the supersaturation value in each of the crystallization experiments undertaken. Supersaturation C^* is defined as $C^* = C/C_0$ where C is the solution concentration and C_0 is the saturated solution concentration.

Crystallization experiments were performed in 20 mL glass vials. A cleaned, glass cover slip was placed at the bottom of four vials, and 10 mL of solution (either 100% H_2O or 75% H_2O) was added to each. Barium chloride solution (0.01 M) was added in order that C^* in each vial was one of the following values, 5, 25, 50, or 100. The four vials were then placed in the bath and allowed to equilibrate (~1 h). Subsequently, Na_2SO_4 solution (0.01 M) was added and the vial cap replaced, and the vial was shaken gently by hand to commence precipitation. The pH for the crystallization experiments was ~6. The vials were then left in the bath for 24 h before removing the glass slide from each of the vials. The excess solution was removed by adsorbing it off using a filter membrane, and the slide was subsequently prepared for scanning electron microscope (SEM) observation.

SEM Procedure. The glass cover slide obtained from the crystallization experiments was placed onto a carbon coated SEM stub, and carbon paint was applied around the slide to ensure electrical contact (this helped in avoiding excessive charging in the SEM). The samples were then dried in a desiccator and gold sputtered before viewing in a Philips XL30 SEM.

Results and Discussion

Molecular Dynamics Simulation of the Barite−Water Interface. MD simulations of the (001), (210), and (010) crystal faces of barite in contact with water were performed. After a brief equilibration period, in all the simulations a structured water layer appears on the crystal surface, as indicated by the water density distribution (Figure 1a−c). This finding is in agreement with X-ray reflectivity experiments that showed the presence of ordered water on the barite crystal surfaces.[44] These water molecules are strongly hydrogen bonded to the surface sulfate oxygen atoms and/or coordinated to the barium atoms.

The overall extent of surface relaxation can be calculated from the displacement of the surface sulfate and barium positions with respect to the bulk lattice (Figure 1a−c). It turns out that little or no surface relaxation (displacement < 0.02 nm) is observed for barium ions. For the sulfate ions, a small relaxation of the outermost layer is observed on the (210) and (001) surfaces (Figure 1a, c) and is related to partial rotation of the exposed surface ions. Again this result is in qualitative agreement with X-ray reflectivity experiments.[44]

The MD averaged surface energies calculated for the (001), (010), and (210) surfaces are 241(18), 193(15), 194(15) mJ m^{-2}, respectively. For the (010) and (210) faces, the surface energies are remarkably similar and smaller than for the (001) surface. A similar result was previously obtained by Jang et al.[22] with two completely different force fields, suggesting that this result is robust with respect to the choice of functional form for the interatomic interactions. However, the relative energies obtained are not consistent with those that would be expected from the morphology of barite crystals grown at low to moderate supersaturation, where the (010) facet is the least morphologically significant, while the remaining two are the dominant crystal faces (Figure 2). This type of interpretation implicitly assumes that the largest faces are the thermodynamically most stable. We therefore conclude that thermodynamics alone cannot explain the morphology of barite crystals and that some kinetic effect must also play a role.

MD Simulation of Nucleation on Barite. To investigate the issue of the kinetics of surface growth, the process of 2D nucleation on the (001), (210), and (010) faces has been studied by performing 100 ns of MD simulation of barite in contact with a 1 M solution of barium sulfate. In the very first steps of the simulation, most of the dissolved Ba^{2+} and SO_4^{2-} ions aggregate to form weakly ordered colloidal particles, and only a few ions remain free in the solution. This is expected, owing to the very high level of initial supersaturation. As a result, the activity of the free ions in solution drops to $\sim 10^{-2}$ M, corresponding to a supersaturation of about 1000.

The ion distribution as a function of the distance from the surface provides an estimate of the probability of finding an ion at a given distance from the surface. Parts a−c of Figure 3 clearly indicate that on the (001) and (210) surfaces there is a barrier that prevents ions from coming closer than approximately 0.3 nm to the surface. This barrier appears to be larger for the barium ions than for the sulfate ions since no barium ion is

(43) Roux, B. *Comput. Phys. Commun.* **1995**, *91*, 275−282.

(44) Fenter, P.; McBride, M. T.; Srajer, G.; Sturchio, N. C.; Bosbach, D. *J. Phys. Chem. B* **2001**, *105*, 8112−8119.

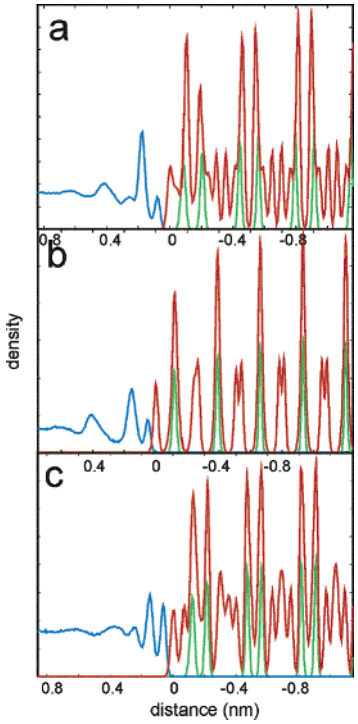

Figure 1. MD simulation of barite−water interfaces. Normalized density of water (blue), sulfate (red), and barium (green) plotted as a function of the position along the *z*-axis of the simulation cell, where *z* is the surface normal direction. Profiles for the (a) (001), (b) (010), and (c) (210) surfaces are reported. Densities are normalized such that the integral of each density over the whole *z*-axis is equal to 1.

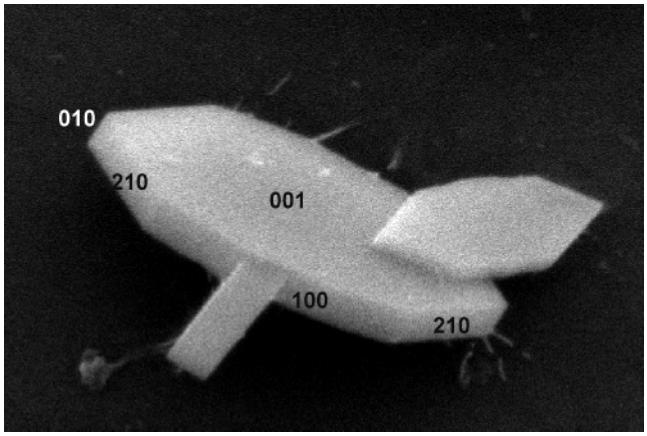

Figure 2. SEM picture of barite crystals grown from aqueous solution at low supersaturation ($C^* = 5$). The morphologically most important crystal faces are indicated.

observed to diffuse to the surface during the 100 ns of dynamical simulation. This finding suggests that the time required for a barium ion to reach the (001) or (210) surfaces may be of the order of microseconds, or longer, and is in line with the prediction, based on the experimental growth rates, that for divalent ion sulfates the desolvation of cations is rate limiting for crystal growth.[23] On the other hand, the sulfate ions that eventually cross the barrier remain trapped on the surface, indicating that, at this supersaturation, the size of a two-dimensional critical nucleus could be as small as a single ion pair and that the barrier to nucleation is largely kinetic.

On the (010) face formation of a crystallization nucleus is observed. During the simulation the nucleus grows in the 001 direction until a periodic row of barium and sulfate ions is

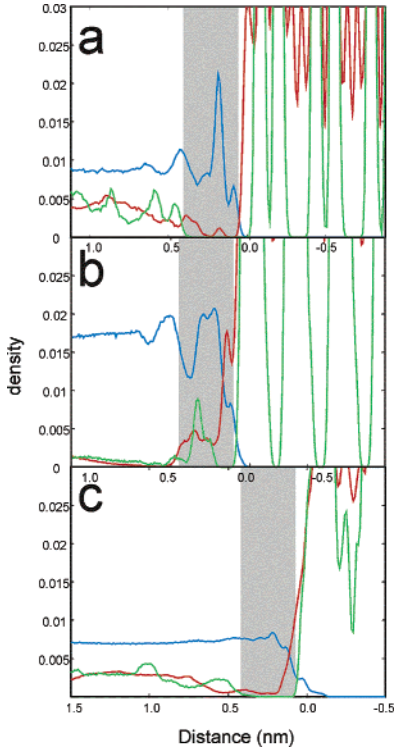

Figure 3. MD simulation of the barite-supersaturated solution interface. Densities of water (blue), sulfate (red), and barium (green) plotted as a function of the position along the *z*-axis of the simulation cell, where *z* is the direction normal to the surface. Profiles for the (a) (001), (b) (010), and (c) (210) surfaces are reported. Densities have been normalized such that the integral over the *z*-axis is equal to 1. The shaded area indicates the region within 0.3 nm from the surface where, in panels a and c, little or no density of ions is observed.

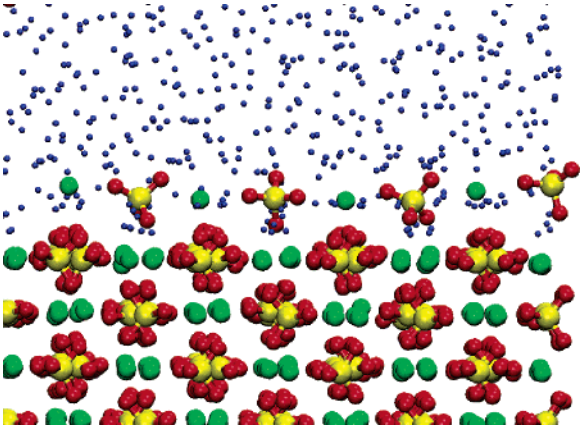

Figure 4. One-dimensional crystallization nucleus formed on the (010) surface of barite after 100 ns of MD simulation. Water molecules are shown as small blue spheres representing the position of oxygen for clarity.

formed. Growth in the other directions is not observed on the time scale of the present simulation (Figure 4).

These calculations show that, despite having the same or lower surface energy, nucleation on the (010) face occurs at a higher rate than for either the (210) or the (001) face. The calculations also suggest that nucleation is limited by a kinetic barrier that prevents the Ba^{2+} from approaching the crystal surface. This barrier has been quantified by performing umbrella sampling molecular dynamics simulations where a Ba^{2+} ion is progressively moved from the bulk solution to the crystal surface (Figure 5). The data obtained from the umbrella sampling simulations were analyzed to calculate reaction free energies.

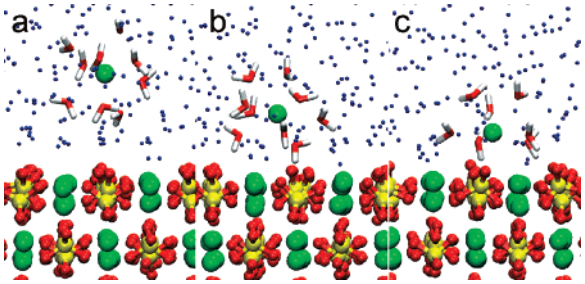

Figure 5. Umbrella sampling simulation of a Ba^{2+} ion approaching the (001) surface of barite: (a) starting position away from the surface, the ion is in a spherical cage of nine water molecules; (b) transition state, the water cage is squeezed as the ion approaches the crystal surface; (c) final state, the ion is now adsorbed on the surface and two of the water molecules have been replaced by sulfate oxygen atoms.

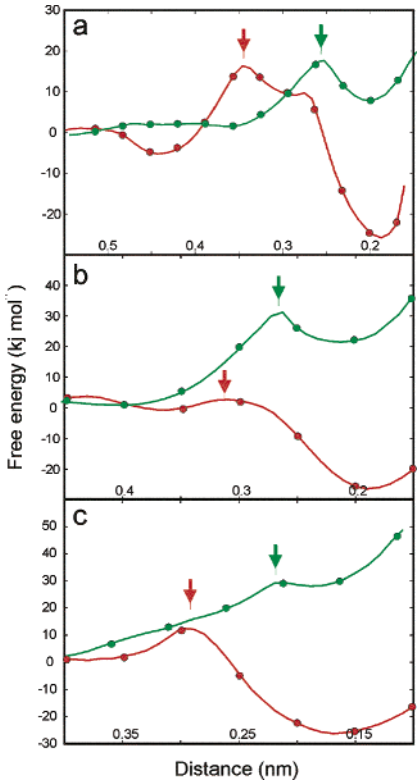

Figure 6. Reaction free energy calculated from the umbrella sampling simulation for the (a) (001), (b) (010), and (c) (210) crystal faces. The free energy was calculated for a clean surface (green line) and in the presence of a sulfate ion (red line). Green and red arrows indicate the position of the kinetic barriers in the two cases. Green and red points indicate the equilibrium position of the constraints in the umbrella sampling simulations.

Activation barriers for approaching a clean surface are determined to be 20, 30, and 30 kJ mol^{-1} for the (001), (010), and (210) faces, respectively (Figure 6a−c). The transition state is located between 0.2 and 0.3 nm from the surface and is related to the reorganization of the water molecules on the crystal surface and around the ion as the ion approaches the surface (Figure 5a−c).

Although formally the rates of cation migration to the surface depend on not only the activation free energy but also the prefactor, we will assume in the subsequent discussion that the dominant influence is likely to be the barrier height. This is on the basis of the magnitude of the activation free energy differences, given the exponential dependence of the rate on these values, and the fact that there is no reason to suppose that the prefactors would differ significantly between the surfaces since these are primarily associated with the motions of the cation in the solution phase.

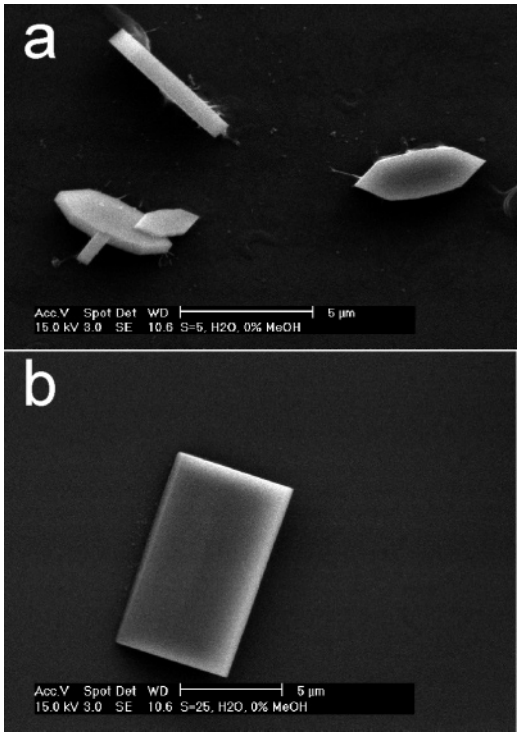

Figure 7. SEM images of barite particles obtained from crystallization in pure water: (a) $C^* = 5$, showing a platelet morphology and (b) $C^* = 25$, showing a single, dominant (*hk*0) face.

The process of cation adsorption alone on the surface is not only activated, but also thermodynamically unfavorable. Therefore, it is very unlikely that a barium ion may adsorb on a clean crystal surface, in agreement with the results of the previous MD simulations. However, when a sulfate ion is on the surface, the barium ion diffuses through the solution until, at low surface distance, a $SO_4^{2-}\cdots Ba^{2+}$ ion pair is formed. As a consequence, the process becomes thermodynamically favored on all faces. Remarkably, on the (010) face the anion is able to assist the cation desolvation to the extent that the kinetic barrier almost vanishes, while on the (001) and (210) surfaces a barrier of 10−20 kJ mol^{-1} is still observed. These results indicate that this assisted desolvation process is highly surface specific.

We conclude that the difference in the rate of nucleation and growth on the (010), (001), and (210) faces is due to the rate of adsorption of Ba^{2+} ions on the crystal surface and this rate is dominated by the process of surface and ion desolvation. This is an activated process on the (001) and (210) faces, but may become diffusion-limited on the (010) face in the presence of sulfate ions that are able to assist the cation desolvation. It is also worth noting that the thermodynamics of Ba^{2+} adsorption on the three surfaces are very similar, and so what makes the rate of nucleation different is an entirely kinetic effect.

Scanning Electron Microscopy of Barium Crystals Grown from a Methanol Solution. The previous findings strictly relate the growth kinetics to the water surface tension. We therefore expect that decreasing the interaction between the surface and the solvent should strongly affect the crystal morphology. To test this hypothesis, barite crystals were grown from both an aqueous solution and a water/methanol mixture, and the resulting crystals were imaged with SEM. Particles were grown from

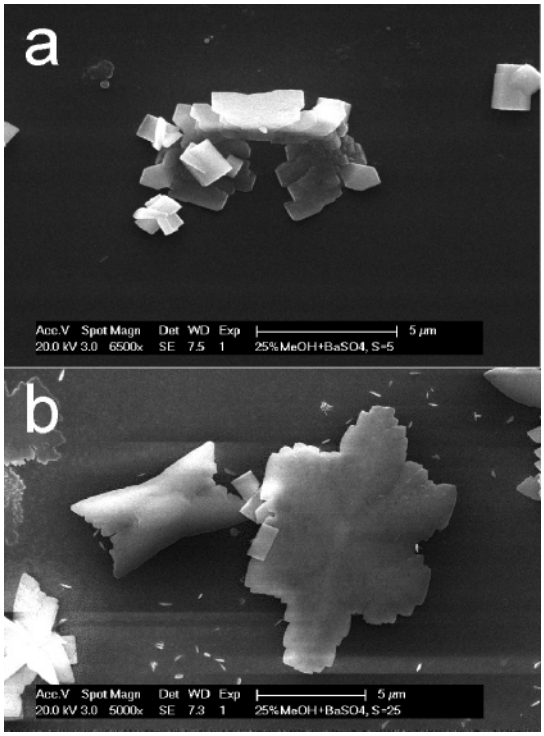

Figure 8. SEM images of barite particles obtained from crystallization in 25% methanol: (a) $C^* = 5$; (b) $C^* = 25$.

aqueous solutions at low (∼5) and moderate (∼25) supersaturation. At $C^* = 5$, 2D nucleation is expected to be rate-limiting for crystal growth, while at $C^* = 25$ the diffusion of steps becomes rate-limiting.[9] The morphology of crystals grown at low supersaturation is platelet-like with dominant (001) faces (Figure 7a). At higher supersaturation ($C^* = 25$), it becomes rectangular, and pillow shaped particles are obtained with rounded (*hk*0) faces dominating the morphology (Figure 7b).

The morphologies of the crystals obtained at low to moderate supersaturation from 25% methanol solutions (Figure 8) are remarkably different from those of the crystals grown from water at the same supersaturation (Figure 7). In particular, the platelet aspect with dominant (001) faces is not observed, and the morphology of the particles obtained from methanol containing solutions resembles crystals grown from water at higher supersaturations.

The above results indicate that even at low supersaturation 2D nucleation may not be rate limiting for crystal growth from methanol solutions, thus providing strong support for the hypothesis, based on MD simulations, that the rate-limiting process for 2D nucleation is related to surface and ion desolvation. This process is faster on the (010) face because of the catalytic properties of the sulfate anions adsorbed on that face.

Conclusions

Molecular dynamics simulations of the barite surface in contact with a supersaturated solution suggest that a key kinetic barrier to nucleation, and therefore crystal growth, at low to moderate supersaturation is the desolvation of the crystal surface and cation. The hypothesis that desolvation of the surface and cations may be a relevant kinetic step is supported by the fact that the morphologies of crystals grown from water/methanol mixtures at low supersaturation are remarkably different from crystals grown from pure water under the same conditions and are similar to crystals grown from water at higher supersaturation, where nucleation is not rate-limiting.

Remarkably, it is found that the anion can assist the process of cation desolvation on specific crystal faces. These are the fastest growing faces of the crystal, despite their thermodynamic stability, which is comparable to the other faces. We conclude that the crystal morphology, at low to moderate supersaturations, is dominated by the kinetics of assisted cation deposition onto the crystal surface. There is no specific reason this type of kinetic control on crystallization should be characteristic of barite only. Indeed, most of the divalent ionic crystals exhibit very similar crystal growth kinetics.[14,21] We therefore suggest that this type of mechanism may be important for the growth of other crystals, such as calcite or apatite. This raises the important issue of whether catalytic desolvation may be used by biological systems as a means to control biomineralization. Our calculations show that this may be indeed possible; further experiments will be required to test this hypothesis on systems of biological relevance.

Acknowledgment. We gratefully acknowledge the support of the ARC for a Fellowship for S.P., the Government of Western Australia for a Premier's Research Fellowship for J.D.G., the Australian Government's Cooperative Research Centre (CRC) Program, through the Parker CRC for Integrated Hydrometallurgy Solutions for support of F.J., and iVEC and APAC for the provision of computing resources. We also thank Andrew Rohl and Donncha Haverty for valuable discussions.

Supporting Information Available: Relationship between methanol content and the barium sulfate equilibrium solubility product. This material is available free of charge via the Internet at http://pubs.acs.org.

JA064706Q